

1 **The Spike Protein S1 Subunit of SARS-CoV-2 Contains an LxxIxE-like Motif that is**  
2 **Known to Recruit the Host PP2A-B56 Phosphatase**

3

4 Halim Maaroufi

5 Institut de biologie intégrative et des systèmes (IBIS). Université Laval. Quebec. Canada

6 [Halim.maaroufi@ibis.ulaval.ca](mailto:Halim.maaroufi@ibis.ulaval.ca)

7

8 **ABSTRACT** The novel betacoronavirus (SARS-CoV-2) is highly contagious and can cause  
9 serious acute respiratory illness syndromes, often fatal, called covid-19. It is an urgent priority to  
10 better understand SARS-CoV-2 infection mechanisms that will help in the development of  
11 prophylactic vaccines and therapeutics that are very important to people health and socioeconomic  
12 stability around the world. The surface coronavirus spike (S) glycoprotein is considered as a key  
13 factor in host specificity because it mediates infection by receptor-recognition and membrane  
14 fusion. Here the analysis of CoV-2 S protein revealed in S1subunit a B56-binding LxxIxE-like  
15 motif that could recruit the host protein phosphatase 2A (PP2A). This motif is absent in SARS-  
16 CoV and MERS-CoV. PP2A is a major family of serine/threonine phosphatases in eukaryotic cells.  
17 Phosphatases and kinases are big players in the regulation of pro-inflammatory responses during  
18 pathogenic infections. Moreover, studies have shown that viruses use multiple strategies to target  
19 PP2A in order to manipulate host's antiviral responses. The latest studies have indicated that  
20 SARS-CoV-2 is involved in sustained inflammation in the host. Therefore, by controlling acute  
21 inflammation; it is possible to eliminate its dangerous effects on the host. Among efforts to fight  
22 covid-19, the interaction between LxxIxE-like motif and PP2A-B56-binding pocket could be a  
23 target for the development of a bioactive peptide and ligand inhibitors for therapeutic purposes.

24

25

26 **KEYWORDS** Coronavirus; SARS-CoV-2; spike S glycoprotein; PP2A-B56 phosphatase;  
27 LxxIxE-like motif; inflammation; therapeutic peptides.

## 28 INTRODUCTION

29

30 In March 11<sup>th</sup> 2020, the World Health Organization (WHO) announced that covid-19 situation is a  
31 pandemic because of the speed and scale of transmission. Coronaviruses (CoVs) are a large family  
32 of enveloped single positive-stranded RNA viruses that can infect both mammalian and avian  
33 species because their rapid mutation and recombination facilitate their adaptation to new hosts  
34 (Graham and Baric, 2010; Li, 2013). They can cause severe, often fatal acute respiratory disease  
35 syndromes named covid-19. CoVs are classified into *Alpha-*, *Beta-*, *Gamma-*, and  
36 *Deltacoronavirus* genetic genera. The novel betacoronavirus (betaCoVs) SARS-CoV-2 is  
37 relatively close to other betaCoVs: severe acute respiratory syndrome coronavirus (SARS-CoV),  
38 Middle East respiratory syndrome coronavirus (MERS-CoV), bat coronavirus HKU4, mouse  
39 hepatitis coronavirus (MHV), bovine coronavirus (BCoV), and human OC43 coronavirus (HCoV-  
40 OC43). SARS-CoV emerged in China (2002–2003) and spread to other countries (more than 8,000  
41 infection cases and a fatality rate of ~10%) (Peiris et al., 2003). In 2012, MERS-CoV was detected  
42 in the Middle East. It spread to multiple countries, infecting more than 1,700 people with a fatality  
43 rate of ~36%.

44 The surface-located SARS-CoV-2 spike glycoprotein S (S) is a 1273 amino acid residues. It is a  
45 homotrimeric, multidomain, and integral membrane protein that give coronaviruses the appearance  
46 of having crowns (*Corona* in Latin) (Li, 2016). It is a key piece of viral host recognition (receptor-  
47 recognition) and organ tropism and induces strongly the host immune reaction (Li, 2015). It is  
48 subdivided to S1 subunit that binds to a receptor on the host cell surface and S2 subunit that permits  
49 viral and host membranes fusion. S1 subunit is divided into two domains, an N-terminal domain  
50 (NTD) and a C-terminal receptor-binding domain (RBD) that can function as viral receptors-  
51 binding (Li, 2012). In addition, S1 subunit is normally more variable in sequence among different  
52 CoVs than is the S2 subunit (Masters, 2006).

53 Protein phosphatase 2A (PP2A) is a major family of serine/threonine phosphatases in eukaryotic  
54 cells and regulates diverse biological processes through dephosphorylation of numerous signaling  
55 molecules. PPA2 and phosphatase 1 (PP1), regulates over 90% of all ser/thr dephosphorylation  
56 events in eukaryotic cells (Eichhorn et al., 2009). PP2A is a heterotrimeric holoenzyme composed  
57 of a stable heterodimer of the scaffold A-subunit (PP2A-A) and catalytic C-subunit (PP2A-C) and  
58 a variable mutually exclusive regulatory subunit from four families (B (B55), B' (B56), B'' and B''')

59 which provide substrate specificity. The human B56 family consists of at least five different  
60 members ( $\alpha$ ,  $\beta$ ,  $\gamma$ ,  $\delta$  and  $\epsilon$ ). Phosphatases and kinases are big players in the regulation of pro-  
61 inflammatory responses during microbial infections. Moreover, studies have revealed that viruses  
62 use multiple strategies to target PP2A in the aim to manipulate host antiviral responses (Guergnon  
63 et al., 2011). Here, face to urgent priority to fight the novel SARS-CoV-2 due to its grave  
64 consequences in the human health and socioeconomic stability around the world, S protein was  
65 analyzed because its importance in mediating infection. This analysis revealed in S1 subunit a B56-  
66 binding LxxIxE-like motif that could recruit the host PP2A. The interaction S1 subunit-host PP2A-  
67 B56 could be a target for the development of a bioactive peptide and ligand inhibitors for  
68 therapeutic purposes.

69

## 70 **RESULTS AND DISCUSSION**

71

### 72 *Two LxxIxE-like motifs in S1 and S2 subunits of Spike S*

73

74 Sequence analysis of SARS-CoV-2 spike protein by the eukaryotic linear motif (ELM) resource  
75 (<http://elm.eu.org/>) revealed short linear motifs (SLiMs) known as LxxIxE-like motif  
76 ,<sup>293</sup>LDPLSE<sup>298</sup> in S1 subunit and <sup>1197</sup>LIDLQE<sup>1202</sup> in S2 subunit (Fig. 1). SLiMs are few amino  
77 acid residues (3-15) in proteins that facilitate protein sequence modifications and protein-protein  
78 interactions (Davey et al., 2012; Van Roey et al., 2014). Viruses are known to mutate quickly and  
79 thus create mimic motifs, on very short time scales, that could hijack biological processes in the  
80 host cell such as cell signaling networks (Davey et al., 2015; Via et al., 2015; Davey et al., 2011).  
81 Interestingly, <sup>293</sup>LDPLSET<sup>299</sup> is only present in SARS-CoV-2 (Fig. 1A). It is absent in the other  
82 coronaviruses S protein analysed in this study. In order to interact with protein(s), <sup>293</sup>LDPLSE<sup>298</sup>  
83 must be present at the surface of S1 subunit. Indeed, it is exposed in the surface of S1 subunit in  
84 the end of NTD (Fig. 3B). Additionally, this motif could be an antigenic epitope to generate  
85 antibodies and/or can help the design of vaccine components and immuno-diagnostic reagents. A  
86 second motif <sup>1197</sup>LIDLQEL<sup>1203</sup> is present in S2 subunit. It is conserved in S2 subunit of SARS-  
87 CoV-2, SARS-CoV, SARS-like of bat from China and Kenya (Fig. 1B). These last  
88 betacoronaviruses are phylogenetically close (Fig. 2). Unfortunately, the region containing  
89 <sup>1197</sup>LIDLQEL<sup>1203</sup> peptide has not been resolved in all known structures of spike S protein of  
90 coronaviruses to know if it is exposed in the surface of S2 subunit.

91 *Interactions of <sup>293</sup>LDPLSET<sup>299</sup> and <sup>1197</sup>LIDLQEL<sup>1203</sup> with Subunit B56-PP2A*

92  
93 To compare the interactions between these peptides and B56 regulatory subunit of PP2A, molecular  
94 docking was performed with the software AutoDock vina (Trott and Olson, 2010). Fig. 4 shows  
95 that peptides are localized in the same region as pS-RepoMan peptide (PDBid: 5SW9) and  
96 important amino acids of LxxIxE-like motif are superposed with those of pS-RepoMan peptide  
97 (Fig. 4C). Interestingly, <sup>293</sup>LDPLSET<sup>299</sup> contains a serine and threonine that could be  
98 phosphorylated generating a negative charge that will interact with positive patch in subunit B56  
99 of PP2A, enhancing binding affinity (Fig. 4A) (Nygren and Scott, 2015). According to Autodock  
100 software, binding affinity of <sup>293</sup>LDPLSET<sup>299</sup> is -4.8 Kcal/mol and this of <sup>1197</sup>LIDLQEL<sup>1203</sup> is -3.5  
101 Kcal/mol. The difference of binding affinity may be explained by the phosphorylation of serine and  
102 threonine. It is known that the binding affinity of SLiMs is relatively weak (low  $\mu$ molar range)  
103 (Gouw et al., 2018). This knowledge of molecular interactions of <sup>293</sup>LDPLSET<sup>299</sup> and B56-PP2A  
104 will pave the way to design a peptide able to mimic the surface of B56-PP2A and strongly bind to  
105 <sup>293</sup>LDPLSET<sup>299</sup> surface precluding PP2A's recruitment (Zaidman and Wolfson, 2016).

106

107 *Protein phosphatase 2A and single RNA viruses*

108  
109 It has been shown in single RNA viruses, Ebola virus (EBOV) and Dengue fever virus (DENV)  
110 that they recruit the host PP2A through its regulatory subunit B56-binding LxxIxE motif to activate  
111 transcription and replication (Kruse et al., 2018; Oliveira et al., 2018). In addition, it has been  
112 shown in mice infected with rhinovirus 1B (the most common viral infectious agent in humans) an  
113 exacerbation of lung inflammation. Administering Salmeterol (beta-agonist) treatment exerts anti-  
114 inflammatory effects by increasing PP2A activity. It is probable that beta-agonists have the  
115 potential to target distinct proinflammatory pathways unresponsive to corticosteroids in patients  
116 with rhinovirus-induced exacerbations. (Hatchwell et al., 2014). It is interesting to learn about  
117 Salmeterol drug and the possibility of using it in covid-19's patients with sustained and dangerous  
118 inflammatory reaction.

## 119 **MATERIALS AND METHODS**

120

### 121 *Sequence analysis*

122

123 To search probable short linear motifs (SLiMs), SARS-CoV-2 spike protein sequence was  
124 scanned with the eukaryotic linear motif (ELM) resource (<http://elm.eu.org/>).

125

### 126 *3D modeling and molecular docking*

127

128 For docking, the coordinates of the <sup>293</sup>LDPLSET<sup>299</sup> peptide were extracted from spike S protein  
129 of CoV-2 structure (PDBid: 6VSB\_A). Unfortunately, the region containing <sup>1197</sup>LIDLQEL<sup>1203</sup>  
130 peptide has not been resolved in all known structures of spike S protein. So, Pep-Fold (Thevenet  
131 et al., 2012) software was used to model *de novo* this peptide. The model quality of the peptide  
132 was assessed by analysis of a Ramachandran plot through PROCHECK (Vaguine et al., 1999).  
133 The docking of the two peptides into regulatory subunit B56 of PPA2 (PDBid: 5SWF\_A) was  
134 performed with the software AutoDock vina (Trott and Olson, 2010). The 3D complex  
135 containing regulatory subunit B56 of PPA2 and peptides was refined by using FlexPepDock  
136 (London et al., 2011), which allows full flexibility to the peptide and side-chain flexibility to the  
137 receptor. The electrostatic potential surface of the regulatory subunit B56 of PPA2 was realized  
138 with PyMOL software (<http://pymol.org/>).

139

### 140 *Phylogeny*

141

142 To establish the phylogenetic relationships between spike S protein of SARS-CoV-2 and  
143 representative betacoronaviruses, amino acid residues sequences were aligned with Clustal  
144 omega (Sievers et al., 2011) and a phylogenetic tree was constructed with MrBayes (Huelsenbeck  
145 and Ronquist, 2001) using: Likelihood model (Number of substitution types: 6(GTR);  
146 Substitution model: Poisson; Rates variation across sites: Invariable + gamma); Markov Chain  
147 Monte Carlo parameters ( Number of generations: 100 000; Sample a tree every: 1000  
148 generations) and Discard first 500 trees sampled (burnin).

149

## 150 **ACKNOWLEDGMENTS**

151 I would like to thank the IBIS bioinformatics group for their assistance.

152

153 **CONFLICT OF INTERESTED**

154 The author declares that he has no conflicts of interest.

155

156

157 **REFERENCES**

158 Davey, N.E., Cyert, M.S., Moses, A.M., 2015. Short linear motifs - ex nihilo evolution of protein  
159 regulation. *Cell Commun. Signal.* 13, 43. <https://doi.org/10.1186/s12964-015-0120-z>.

160

161 Davey, N.E., Travé, G., Gibson, T.J., 2011. How viruses hijack cell regulation. *Trends Biochem.*  
162 *Sci.* 36, 159–169. <https://doi.org/10.1016/j.tibs.2010.10.002>

163

164 Davey, N.E., Van Roey, K., Weatheritt, R.J., Toedt, G., Uyar, B., Altenberg, B., Budd, A.,  
165 Diella, F., Dinkel, H., Gibson, T.J., 2012. Attributes of short linear motifs. *Mol. Biosyst.* 8, 268–  
166 281. <https://doi.org/10.1039/c1mb05231d>

167

168 Eichhorn, P.J.A., Creighton, M.P., Bernards, R., 2009. Protein phosphatase 2A regulatory  
169 subunits and cancer. *Biochim. Biophys. Acta* 1795, 1–15.

170 <https://doi.org/10.1016/j.bbcan.2008.05.005>

171

172 Gouw, M., Michael, S., Sámano-Sánchez, H., Kumar, M., Zeke, A., Lang, B., Bely, B., Chemes,  
173 L.B., Davey, N.E., Deng, Z., Diella, F., Gürth, C.-M., Huber, A.-K., Kleinsorg, S., Schlegel, L.S.,  
174 Palopoli, N., Roey, K.V., Altenberg, B., Reményi, A., Dinkel, H., Gibson, T.J., 2018. The  
175 eukaryotic linear motif resource - 2018 update. *Nucleic Acids Res.* 46, D428–D434.

176 <https://doi.org/10.1093/nar/gkx1077>

177

178 Graham, R.L., Baric, R.S., 2010. Recombination, reservoirs, and the modular spike: mechanisms  
179 of coronavirus cross-species transmission. *J. Virol.* 84, 3134–3146.

180 <https://doi.org/10.1128/JVI.01394-09>

181

182 Guernon, J., Godet, A.N., Galioot, A., Falanga, P.B., Colle, J.-H., Cayla, X., Garcia, A., 2011.  
183 PP2A targeting by viral proteins: a widespread biological strategy from DNA/RNA tumor viruses  
184 to HIV-1. *Biochim. Biophys. Acta* 1812, 1498–1507.

185 <https://doi.org/10.1016/j.bbadis.2011.07.001>

186

187 Hatchwell, L., Girkin, J., Dun, M.D., Morten, M., Verrills, N., Toop, H.D., Morris, J.C.,  
188 Johnston, S.L., Foster, P.S., Collison, A., Mattes, J., 2014. Salmeterol attenuates chemotactic  
189 responses in rhinovirus-induced exacerbation of allergic airways disease by modulating protein  
190 phosphatase 2A. *J. Allergy Clin. Immunol.* 133, 1720–1727.

191 <https://doi.org/10.1016/j.jaci.2013.11.014>

192

193 Huelsenbeck, J.P., Ronquist, F., 2001. MRBAYES: Bayesian inference of phylogenetic trees.  
194 *Bioinformatics* 17, 754–755. <https://doi.org/10.1093/bioinformatics/17.8.754>

195  
196 Kruse, T., Biedenkopf, N., Hertz, E.P.T., Dietzel, E., Stalman, G., López-Méndez, B., Davey,  
197 N.E., Nilsson, J., Becker, S., 2018. The Ebola Virus Nucleoprotein Recruits the Host PP2A-B56  
198 Phosphatase to Activate Transcriptional Support Activity of VP30. *Mol. Cell* 69, 136–145.e6.  
199 <https://doi.org/10.1016/j.molcel.2017.11.034>  
200  
201 Li, F., 2016. Structure, Function, and Evolution of Coronavirus Spike Proteins. *Annu Rev Virol*  
202 3, 237–261. <https://doi.org/10.1146/annurev-virology-110615-042301>  
203 Li, F., 2015. Receptor recognition mechanisms of coronaviruses: a decade of structural studies. *J.*  
204 *Virol.* 89, 1954–1964. <https://doi.org/10.1128/JVI.02615-14>  
205  
206 Li, F., 2013. Receptor recognition and cross-species infections of SARS coronavirus. *Antiviral*  
207 *Res.* 100, 246–254. <https://doi.org/10.1016/j.antiviral.2013.08.014>  
208  
209 Li, F., 2012. Evidence for a common evolutionary origin of coronavirus spike protein receptor-  
210 binding subunits. *J. Virol.* 86, 2856–2858. <https://doi.org/10.1128/JVI.06882-11>  
211  
212 London, N., Raveh, B., Cohen, E., Fathi, G., Schueler-Furman, O., 2011. Rosetta FlexPepDock  
213 web server--high resolution modeling of peptide-protein interactions. *Nucleic Acids Res.* 39,  
214 W249–53. <https://doi.org/10.1093/nar/gkr431>  
215  
216 Masters, P.S., 2006. The molecular biology of coronaviruses. *Adv. Virus Res.* 66, 193–292.  
217 [https://doi.org/10.1016/S0065-3527\(06\)66005-3](https://doi.org/10.1016/S0065-3527(06)66005-3)  
218  
219 Nygren, P.J., Scott, J.D., 2015. Therapeutic strategies for anchored kinases and phosphatases:  
220 exploiting short linear motifs and intrinsic disorder. *Front. Pharmacol.* 6, 158.  
221 <https://doi.org/10.3389/fphar.2015.00158>  
222  
223 Oliveira, M., Lert-Itthiporn, W., Cavadas, B., Fernandes, V., Chuansumrit, A., Anunciação, O.,  
224 Casademont, I., Koeth, F., Penova, M., Tangnaratchakit, K., Khor, C.C., Paul, R., Malasit, P.,  
225 Matsuda, F., Simon-Lorière, E., Suriyaphol, P., Pereira, L., Sakuntabhai, A., 2018. Joint ancestry  
226 and association test indicate two distinct pathogenic pathways involved in classical dengue fever  
227 and dengue shock syndrome. *PLoS Negl. Trop. Dis.* 12, e0006202.  
228 <https://doi.org/10.1371/journal.pntd.0006202>  
229  
230 Peiris, J.S.M., Lai, S.T., Poon, L.L.M., Guan, Y., Yam, L.Y.C., Lim, W., Nicholls, J., Yee,  
231 W.K.S., Yan, W.W., Cheung, M.T., Cheng, V.C.C., Chan, K.H., Tsang, D.N.C., Yung, R.W.H.,  
232 Ng, T.K., Yuen, K.Y., SARS study group, 2003. Coronavirus as a possible cause of severe acute  
233 respiratory syndrome. *Lancet* 361, 1319–1325. [https://doi.org/10.1016/s0140-6736\(03\)13077-2](https://doi.org/10.1016/s0140-6736(03)13077-2)  
234  
235 Sievers, F., Wilm, A., Dineen, D., Gibson, T.J., Karplus, K., Li, W., Lopez, R., McWilliam, H.,  
236 Remmert, M., Söding, J., Thompson, J.D., Higgins, D.G., 2011. Fast, scalable generation of high-  
237 quality protein multiple sequence alignments using Clustal Omega. *Mol. Syst. Biol.* 7, 539.  
238 <https://doi.org/10.1038/msb.2011.75>  
239  
240 Thévenet, P., Shen, Y., Maupetit, J., Guyon, F., Derreumaux, P., Tufféry, P., 2012. PEP-FOLD:

241 an updated de novo structure prediction server for both linear and disulfide bonded cyclic  
242 peptides. *Nucleic Acids Res.* 40, W288–93. <https://doi.org/10.1093/nar/gks419>  
243  
244 Trott, O., Olson, A.J., 2010. AutoDock Vina: improving the speed and accuracy of docking with  
245 a new scoring function, efficient optimization, and multithreading. *J. Comput. Chem.* 31, 455–  
246 461. <https://doi.org/10.1002/jcc.21334>  
247  
248 Vaguine, A.A., Richelle, J., Wodak, S.J., 1999. SFCHECK: a unified set of procedures for  
249 evaluating the quality of macromolecular structure-factor data and their agreement with the  
250 atomic model. *Acta Crystallogr. D Biol. Crystallogr.* 55, 191–205.  
251 <https://doi.org/10.1107/S0907444998006684>  
252  
253 Van Roey, K., Uyar, B., Weatheritt, R.J., Dinkel, H., Seiler, M., Budd, A., Gibson, T.J., Davey,  
254 N.E., 2014. Short linear motifs: ubiquitous and functionally diverse protein interaction modules  
255 directing cell regulation. *Chem. Rev.* 114, 6733–6778. <https://doi.org/10.1021/cr400585q>  
256  
257 Via, A., Uyar, B., Brun, C., Zanzoni, A., 2015. How pathogens use linear motifs to perturb host  
258 cell networks. *Trends Biochem. Sci.* 40, 36–48. <https://doi.org/10.1016/j.tibs.2014.11.001>  
259  
260 Wang, X., Bajaj, R., Bollen, M., Peti, W., Page, R., 2016. Expanding the PP2A Interactome by  
261 Defining a B56-Specific SLiM. *Structure* 24, 2174–2181.  
262 <https://doi.org/10.1016/j.str.2016.09.010>  
263  
264 Zaidman, D., Wolfson, H.J., 2016. PinaColada: peptide–inhibitor ant colony ad-hoc design  
265 algorithm. *Bioinformatics* 32, 2289–2296. <https://doi.org/10.1093/bioinformatics/btw133>  
266



267 **Figures**

268

269 **Figure 1.** Multiple alignment of the spike glycoprotein of betacoronaviruses using Clustal omega  
270 (Sievers et al., 2011). LxxIxE-like motifs are indicated by green stars. Numbers at the start of  
271 each sequence corresponding to the GenBank and UniProt accession number. Green stars  
272 indicated LxxIxE-like motif. The figure was prepared with ESPrpt (<http://esprpt.ibcp.fr>).

273

274 **Figure 2.** Unrooted phylogenetic tree of spike protein of representative betacoronaviruses. The  
275 tree was constructed using Mr Bayes method (Huelsenbeck and Ronquist, 2001) based on the  
276 multiple sequence alignment by Clustal omega (Sievers et al., 2011). Numbers at the start of each  
277 sequence corresponding to the GenBank and UniProt accession number. Red rectangle assembles  
278 betacoronaviruses with the same <sup>1197</sup>LIDLQE<sup>1202</sup>. Green star indicated the only betacoronavirus  
279 with <sup>293</sup>LDPLSE<sup>298</sup>.

280

281 **Figure 3.** (A) Diagram representation of the S1 subunit of spike protein of SARS-CoV-2 colored  
282 by domain. N-terminal domain (NTD, cyan), receptor-binding domain (RBD, green), subdomains  
283 1 and 2 (SD1-2, orange) and the localization of <sup>293</sup>LDPLSE<sup>298</sup> in the end of NTD.  
284 (B) Surface structure representation of the S1 subunit of spike protein (PDBid: 6VSB\_A).  
285 <sup>293</sup>LDPLSE<sup>298</sup> peptide is localized in the surface (red).

286

287 **Figure 4.** Electrostatic potential surface representation of the region of the regulatory subunit  
288 B56 of PP2A (PDBid: 5SWF\_A) with docked peptides. (A) <sup>293</sup>LDPLpSEpT<sup>299</sup> (green), (B)  
289 <sup>1197</sup>LIDLQEL<sup>1203</sup> (cyan) and (C) <sup>293</sup>LDPLpSEpT<sup>299</sup> superposed to pS-RepoMan  
290 (<sup>581</sup>RDIASKKPLLpSPIPELPEVPE<sup>601</sup>) peptide (orange, PDBid: 5SW9\_B). The surfaces are colored  
291 by electrostatic potential with negative charge shown in red and positive charge in blue. Images  
292 were generated using PyMol ([www.pymol.org](http://www.pymol.org)).

293

294

**A**

	270	280	290	300	310	320
YP_009724390.1_Human_SARS-CoV-2_Wuhan-Hu-1_China	VGYIQPR	TFLLKY	NENCTITD	AVDCALDP	LSETKCT	LKFTVEKGIYQTSNFRVQPTES
P59594.1_Human_SARS-Cov_HongKong_China	VGYLKPT	TFMLKY	DENCTITD	AVDCSQNP	LAEKCSVK	SFEIDKGIYQTSNFRVVP
ATO98205.1_Bat_SARS-like_coronavirus_China	VGYLKPA	TFMLKY	DENCTITD	AVDCSQNP	LAEKCSVK	SFEIDKGIYQTSNFRVAP
APO40579.1_Bat_SARS-like_coronavirus_Kenya	VGHLLKPL	TMLAEF	DENCTITD	AVDCSQDP	LSEKCT	TKSLTVEKGIYQTSNFRVSP
P36334_Human_SPIKE_CVHOC_coronavirus_OC43	VTFLLTSR	QYLLAF	NQDCVIFNAE	DCMSDF	MSEIKCKTQ	SIAPPTGVYELNGYTVQPIADV
P25190_Bovine_SPIKE_CVBF_coronavirus_strain_F15	VTFLLTSR	QYLLAF	NQDCVIFNAE	DCMSDF	MSEIKCKTQ	SIAPPTGVYELNGYTVQPIADV
P11225_Murine_SPIKE_CVMJH_coronavirus_JHM	VTFLLTSR	QYLLAF	NQDCVIFNAE	DCMSDF	MSEIKCKTQ	SIAPPTGVYELNGYTVQPIADV
ALK80251.1_Human_MERS-CoV_South-Korea	VYKLLQPL	TFLLDF	SVDGYIRRAID	CGFND	LSQLHCSYE	SFDVESGVYVSSFEAKP
A3EX94_Bat_SPIKE_BCHK4_coronavirus_HKU4	VYKLLHQL	TYLLDF	SVDGYIRRAID	CGHDD	LSQLHCSY	SFDVDTGVYVSSFEASAT
QGA70702.1_Erinaceus_coronavirus_HKU31_China	TYQLHKL	NYLVEF	DVGCYIVRAS	DCGANDY	TQLQCSY	GFDMNSGVYVSSFEAN

295

296

**B**

	1190	1200	1210	1220	1230	1240
YP_009724390.1_Human_SARS-CoV-2_Wuhan-Hu-1_China	NEVAKN	LNESL	IDLQEL	GKYEQYIK	KWPWYI	WVGFIAGLIAIVMVTIMLCMTSCCSCLKG
P59594.1_Human_SARS-Cov_HongKong_China	NEVAKN	LNESL	IDLQEL	GKYEQYIK	KWPWYV	WVGFIAGLIAIVMVTIILLCMTSCCSCLKG
ATO98205.1_Bat_SARS-like_coronavirus_China	NEVAKN	LNESL	IDLQEL	GKYEQYIK	KWPWYV	WVGFIAGLIAIVMVTIILLCMTSCCSCLKG
APO40579.1_Bat_SARS-like_coronavirus_Kenya	NEIAKN	LNESL	IDLQEL	GKYEQYIK	KWPWYV	WGVAGIVAIVLMSVIMLCMTSCCSCLKG
P36334_Human_SPIKE_CVHOC_coronavirus_OC43	QEAIKV	LNQSY	INLKD	IGTYEY	VKWPWYV	WVLLICLAGVAMLVLLFFICCTGCGTSCFK
P25190_Bovine_SPIKE_CVBF_coronavirus_strain_F15	QEAIKV	LNQSY	INLKD	IGTYEY	VKWPWYV	WVLLICLAGVAMLVLLFFICCTGCGTSCFK
P11225_Murine_SPIKE_CVMJH_coronavirus_JHM	QEAIKV	LNQSY	INLKD	IGTYEY	VKWPWYV	WVLLICLAGVAMLVLLFFICCTGCGTSCFK
ALK80251.1_Human_MERS-CoV_South-Korea	QQVVK	LNESY	IDLKE	LGNYTY	NKWPWYI	WVGFIAGLVALALCVFFILCCTGCGTNCMG
A3EX94_Bat_SPIKE_BCHK4_coronavirus_HKU4	QEVVK	LNDSY	IDLKE	LGNYTY	NKWPWYV	WVGFIAGLVALLLCVFFILCCTGCGTSCMG
QGA70702.1_Erinaceus_coronavirus_HKU31_China	QSVVEA	LNQSY	IELKEL	GNITY	NKWPWYV	WVGFIAGLVALALCLFFILCCTGCGTSCMG

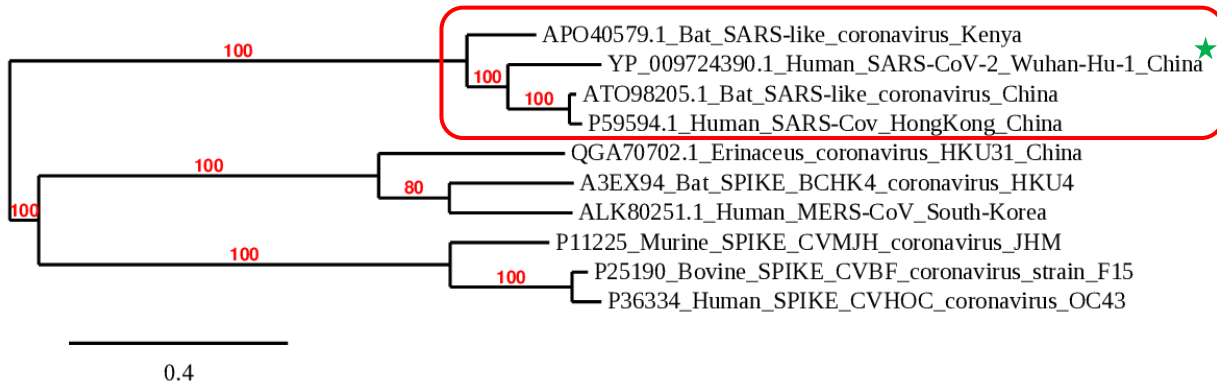
297

298 **Fig. 1**

299

300

1197 **LIDLQEL** 1203



301

302 **Fig. 2**

303

304

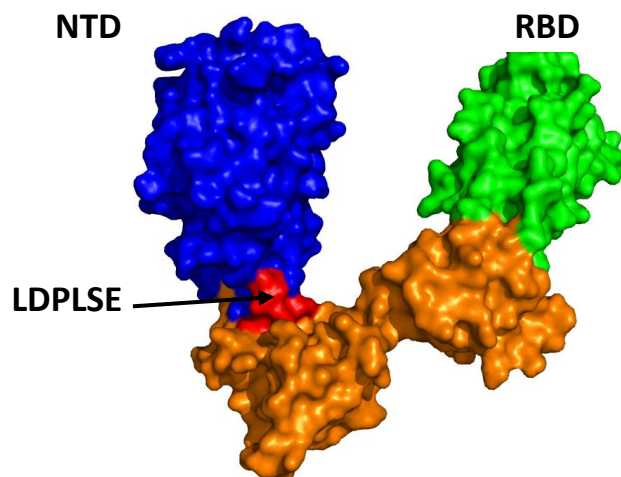
**A**



305

306

**B**



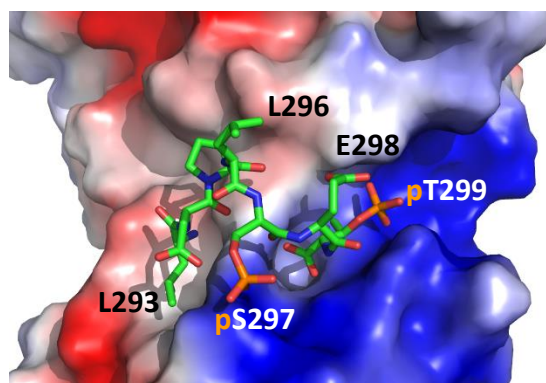
307

308 **Fig. 3**

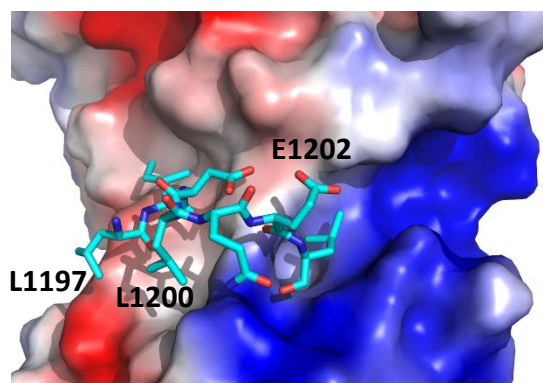
309

310

A



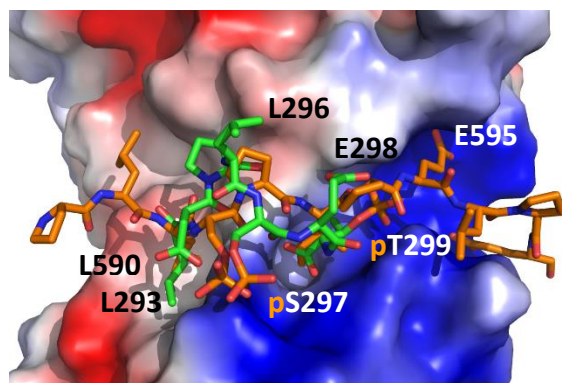
B



311

312

C



313

314

315 **Fig. 4**